PRODUÇÃO ONLINE
REVISTA CIENTÍFICA ELETRÔNICA DE ENGENHARIA DE PRODUÇÃO
ISSN 1676-1901
ABEPRO

ANALYSIS OF THE EFFECTS OF REGION AND DIRECTION ON THE MECHANICAL STRENGTH OF POLYURETHANE FOAMS IN WHITE GOODS REFRIGERATORS

ANÁLISE DOS EFEITOS DA REGIÃO E DIREÇÃO NA RESISTÊNCIA MECÂNICA DE ESPUMAS DE POLIURETANO EM REFRIGERADORES DE LINHA BRANCA

João Paulo Soares Kaiser* E-mail: joaopskaiser@ufpr.br
João Morais da Silva Neto* E-mail: joaomsn@ufpr.br
Harrison Lourenço Corrêa* E-mail: harrisoncorrea@ufpr.br
*Federal University of Paraná (UFPR), Curitiba, Paraná, Brasil.

Abstract: This research focuses on investigating the mechanical properties of polyurethane foam, specifically in the context of the refrigeration industry. Tensile, compression, and flexural tests were conducted to gather comprehensive data on the foam's mechanical behavior under various loading conditions. Samples were collected from different regions within a specific cabinet model to analyze the effects of region and direction of the foam growth on the foam's mechanical properties. The results revealed that samples collected from the top of the cabinet exhibited superior performance compared to those obtained from the bottom. The foam demonstrated isotropic behavior under compression, while exhibiting anisotropic behavior under tensile and flexure. When aligned parallel to the foam growth, the foam displayed slightly higher maximum stress in the tensile and flexural tests. However, the compression test showed comparable strength in both directions. These findings contribute to a better understanding and utilization of PU foam in various industrial sectors, particularly in refrigeration. The data obtained from this research can support the optimization of project designs and facilitate the development of more efficient and economically viable solutions.

Keywords: Polyurethane foam. Mechanical properties. Refrigeration industry.

Resumo: Esta pesquisa concentra-se na investigação das propriedades mecânicas da espuma de poliuretano, especificamente no contexto da indústria de refrigeração. Foram realizados testes de tração, compressão e flexão para coletar dados abrangentes sobre o comportamento mecânico da espuma sob várias condições de carga. Amostras foram coletadas de diferentes regiões dentro de um modelo específico de gabinete para analisar os efeitos da região e da direção do crescimento da espuma nas propriedades mecânicas da espuma. Os resultados revelaram que as amostras coletadas na parte superior do gabinete apresentaram desempenho superior em comparação com aquelas obtidas na parte inferior. A espuma demonstrou comportamento isotrópico sob compressão, enquanto exibia comportamento anisotrópico sob tração e flexão. Quando alinhada paralelamente ao crescimento da espuma, a espuma apresentou um ligeiro aumento na tensão máxima nos testes de tração e flexão. No entanto, o teste de compressão mostrou resistência comparável em ambas as direções. Essas descobertas contribuem para uma melhor compreensão e utilização da espuma de PU em diversos setores industriais, especialmente na refrigeração. Os dados obtidos nesta pesquisa podem apoiar a

otimização de projetos e facilitar o desenvolvimento de soluções mais eficientes e economicamente viáveis.

Palavras-chave: Espuma de poliuretano. Propriedades mecânicas. Indústria de refrigeração.

1 INTRODUCTION

Polyurethanes (PU) are versatile and widely used polymeric material with diverse applications across industries, such as mattresses, coatings, insulation, and toys (American Chemistry Council, Inc., 2021). The discovery of diisocyanate addition polymerization in 1937 by Dr. Otto Bayer and his team marked a significant milestone in the utilization of polyurethane in the United States, leading to a substantial increase in production and economic value over the years (lee; Ramesh, 2004). The industrial importance of polyurethane foams lies in their low density, ease of processing, low thermal conductivity, sound absorption properties, high specific mechanical strength, and adhesive characteristics. As a result, their significance has continued to grow, driven by advancements in plastic technologies (Lee *et al.*, 2017; Kim *et al.*, 2017).

Within the global polymer market, PU holds the sixth position in terms of market size and is characterized by its division into five main categories: foams, coatings, elastomers, adhesives, and other applications. This segmentation emphasizes the wide-ranging adaptability and extensive utilization of PU across various industries, highlighting its diverse scope of applications. Notably, the foam sector constitutes approximately 65% of the overall distribution (Peyrton; Avérous, 2021).

However, despite the widespread use of PU foam, there are still knowledge gaps regarding its mechanical properties and performance in structural applications. This research aims to bridge this gap by investigating the mechanical properties of PU foam, with a specific focus on its viability in the refrigeration industry. Tensile, compression, and flexural testing will be conducted to gather precise data on the mechanical behavior of PU foam under different loading conditions. Additionally, the influence of region and direction factors will be analyzed, and a comparative assessment with other materials commonly used in structural applications will be carried out. Nonetheless, the results obtained are expected to provide valuable insights for a better understanding and enhanced utilization of PU foam in various industrial sectors, contributing to the development of more efficient and economically viable solutions.

Polyurethanes (PU) are versatile and widely used polymeric material with diverse applications across industries, such as mattresses, coatings, insulation, and toys (American Chemistry Council, Inc., 2021). The discovery of diisocyanate addition polymerization in 1937 by Dr. Otto Bayer and his team marked a significant milestone in the utilization of polyurethane in the United States, leading to a substantial increase in production and economic value over the years (Lee; Ramesh, 2004). The industrial importance of polyurethane foams lies in their low density, ease of processing, low thermal conductivity, sound absorption properties, high specific mechanical strength, and adhesive characteristics. As a result, their significance has continued to grow, driven by advancements in plastic technologies (Lee *et al.*, 2017; Kim *et al.*, 2017).

1.1 Objectives

The objective of this research is to comprehensively investigate and evaluate the mechanical characteristics of PU foams employed in commercial white goods refrigerators.

To achieve this objective, the study will be divided into several specific goals. Firstly, a comprehensive literature review will be conducted to provide a sound rationale for the utilization of polyurethane foam in commercial refrigerators. Secondly, the mechanical characterization of PU foams will be performed using standardized testing protocols, enabling a deeper understanding of their mechanical behavior under various loading conditions such as tension, compression, and flexure. Lastly, the investigation will focus on analyzing the influence of region and direction factors on the strength and mechanical properties of PU foam. By pursuing these specific objectives, the study seeks to contribute valuable insights to the scientific knowledge base and facilitate advancements in the application of PU foam in structural contexts.

2 LITERATURE REVIEW

2.1 The polyurethanes

Polyurethanes are typically synthesized through the reaction between a polyol and an isocyanate. A polyol is an organic compound containing multiple hydroxyl groups, while an isocyanate is a molecule composed of nitrogen, carbon, and oxygen. Due to the vast range of available isocyanates and polyols for PU production, a diverse array of materials and properties can be achieved (American Chemistry Council, Inc. , 2021).

Polyurethane foams are manufactured by incorporating polyol and isocyanate, along with an expansion agent. The expansion agent is commonly introduced into the polyol mixture together with other constituents. The polyaddition reaction ensues upon the amalgamation of polyol and isocyanate. The exothermic nature of the polyaddition reaction facilitates the utilization of a fraction of the released heat to volatilize the expansion agents, thereby resulting in the formation of foam (Kapps, 2004).

Polyurethane foams can be classified into two categories: flexible foams with open cells and rigid foams with closed cells. Chemically, both foam types are similar, with variations arising from the type and extent of polymerization, leading to diverse products and properties. Among these categories, rigid PU foams are primarily employed for insulation purposes in refrigerators, making them the focus of this study. Additionally, they find applications in various sectors such as construction, transportation, and pipelines (Peyrton; Avérous, 2021).

2.2 Properties of PU Foams

2.2.1 Compression Behavior of PU Foam

Typically, foams are mechanically analyzed through compression tests. The compressive strength of the material depends on its density, homogeneity, and cell size, with rigid PU foams exhibiting the highest values for this property (Peyrton; Avérous, 2021).

The mechanical behavior or response of PU foams under compression can exhibit two types of behavior, as exemplified by ASTM D1621 (2016) in Figure 1.

Figure 1 - Representation of compression curve points

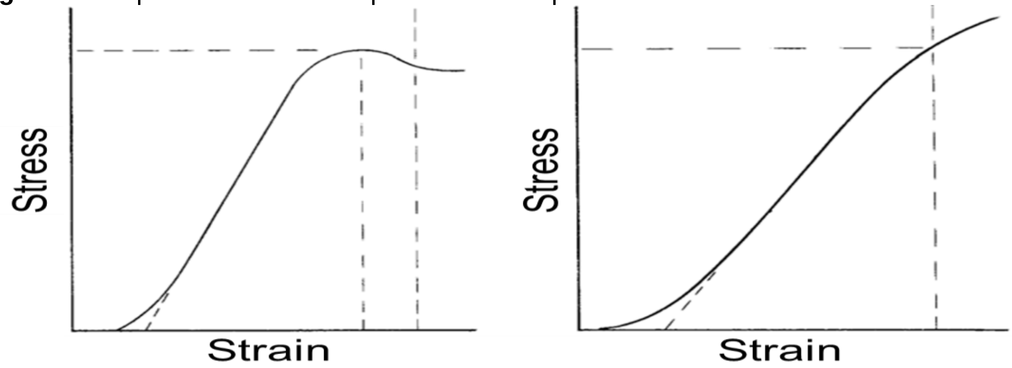

Source: Adapted from ASTM D1621 (2016).

The first behavior can be divided into three regions (Linear Elastic, Plateau, and Densification), as illustrated in Figure 2. In the first region, linear elastic, the flexion and elongation of the cellular structures and the compression of gases occur. In the subsequent stage, plateau region, plastic deformation and rupture of these cellular structures occur, resulting in a drop in stress. Finally, densification occurs as the collapsed cells are compacted on top of each other, as represented in Figure 3 (Kim *et al.*, 2017; Lee *et al.*, 2017).

Figure 2 - Representation of the compression behavior of PU foams

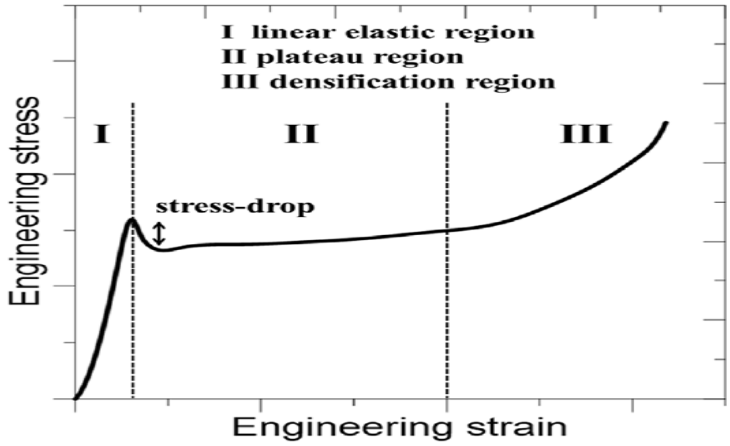

Source: Lee *et al.* (2017).

Figure 3 - Reproduction of the compression behavior of PU foams. Deformation: (a) 4%, (b) 25%, (c) 50%, and (d) 75%

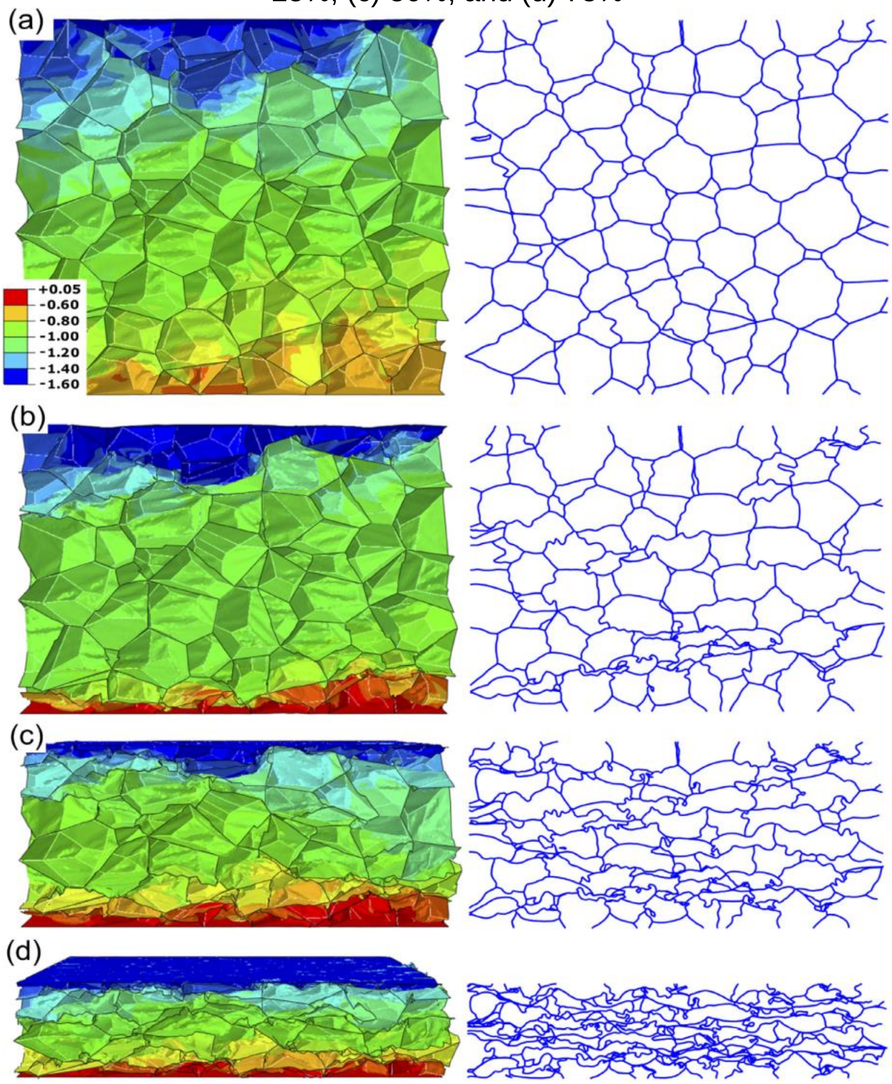

Source: Marvi-Mashhadi, Lopes and LLorca (2020).

In the study conducted by Xu *et al.* (2022), a compression experiment was performed on polyurethane foam with a density of 41,7 kg/m³. The study analyzed the behavior parallel and normal to the foam growth. Additionally, the article demonstrated compliance with the two behavior patterns established by the ASTM D1621 (2016). The sample under compression test is depicted in Figure 4, while the corresponding curves for the two observed behaviors are presented in Figure 5.

Figure 4 - Example of a sample under compression test

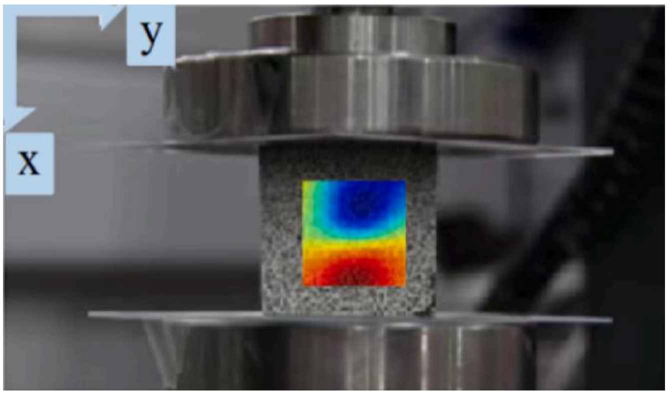

Source: Xu *et al.* (2022).

Figure 5 - Example of curves obtained from the compression test

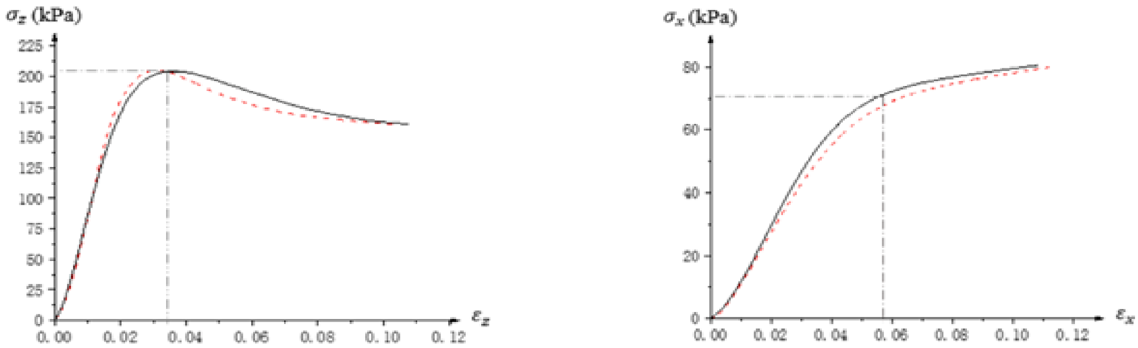

Source: Xu *et al.* (2022).

2.2.2 Tensile behavior of PU Foam

The analysis of PU foam under tension is a topic that has been addressed in a limited number of available studies. Among the consulted articles, it is observed that the testing procedure recommended by ASTM D1623 (2017) is not followed.

In a study conducted by Xu *et al.* (2022), the authors investigated the tensile properties of polyurethane foam with a density of 41.7 kg/m³. The researchers employed samples with dimensions as illustrated in Figure 6. To ensure secure fixation of the PU samples, two aluminum plates were used along with the standard gripping device for tension.

Figure 6 - Example of a sample for tensile testing using aluminum plates

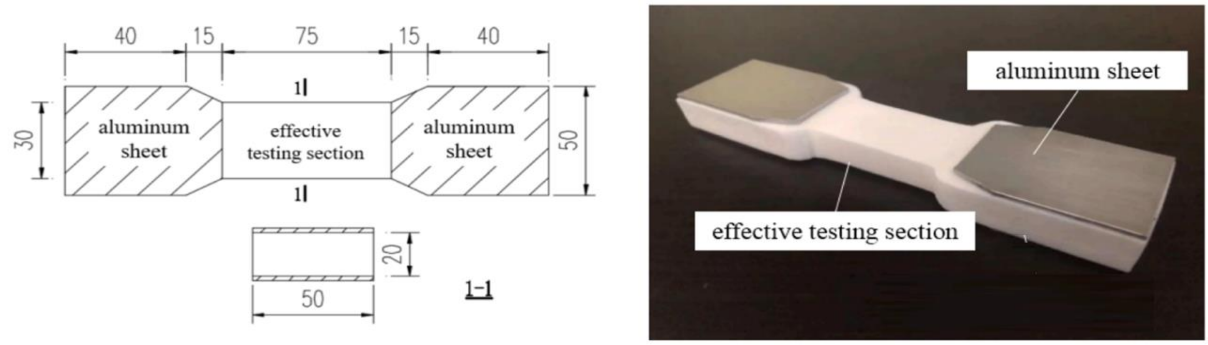

Source: Xu *et al.* (2022).

An additional example presented by Caliri Junior (2010) involves conducting a tensile test on PVC foam with a density of 60 kg/m³. In this context, the author follows the guidelines established by the ASTM D1623 standard (2017), although different specimen geometries were adopted. Additionally, the author employs a rigid substrate that is bonded to the PVC foam using a commercially known adhesive called Araldite, which consists of a resin and a hardener. This configuration allows for the fixation of the substrate to the grip used in the tensile test.

The third example, conducted by Witkiewicz and Zieliński (2006), aimed to examine the behavior of PU foam with a density of 62 kg/m³ under tension. In this approach, the PU samples were cut and subsequently directly fixed to the grips of the tensile testing machine. Figure 7 illustrates the experimental setup employed.

Figure 7 - Example of equipment and sample for tensile testing

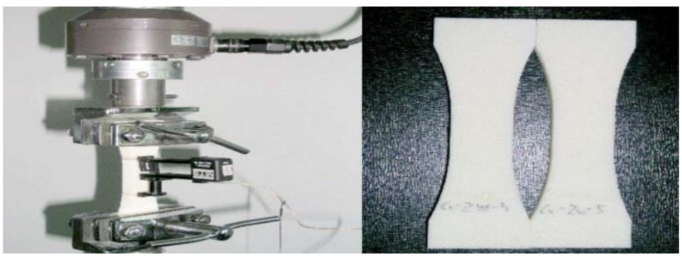

Source: Witkiewicz and Zieliński (2006).

However, due to the inconsistency of evaluation parameters, both in terms of sample geometry and testing methods employed, it becomes unfeasible to make a precise and reliable comparison between the results.

2.2.3 Flexural behavior of PU foam

In the context of flexural behavior, most scientific articles address studies involving sandwich structures (a type of composite structure consisting of two rigid outer layers separated by a lightweight and low-density core), with a scarcity of research specifically addressing the analysis of pure polyurethane (PU) foam behavior. Additionally, it is important to note that, in this specific case, due to the ease of test application, the geometries and procedures adopted are similar both in the ASTM D790 (2003) and in the found studies.

An example of a study related to the measurement of flexural strength using the three-point method is presented by Voiconi *et al.* (2013). In this study, the test was conducted on PU foam samples with three different densities: 100, 145, and 300 kg/m³. Figure 8 illustrates the test configuration and the stress-strain curve obtained from the experiments conducted.

Figure 8 - Example of a three-point flexural test and obtained curves

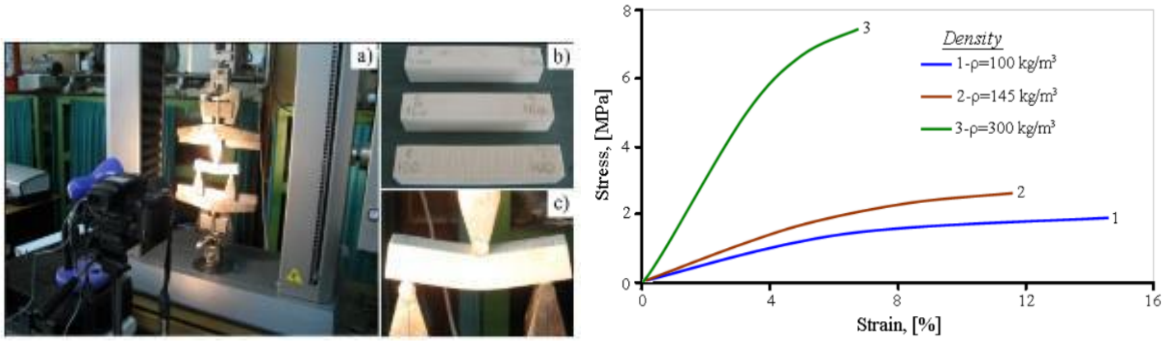

Source: Voiconi *et al.* (2013).

2.2.4 Anisotropy

An isotropic material possesses uniform physical properties in all directions, whereas an anisotropic material exhibits distinct properties depending on the direction of measurement (Callister and Rethwisch, 2014). However, no specific property difference value has been found that is universally accepted to determine whether a material is isotropic or anisotropic. The standards employed in this study recommend conducting tests to identify anisotropic behavior if suspicions arise.

The term degree of anisotropy is employed to quantify the variation between different directions, expressed as the ratio of measured properties along each direction. This ratio ranges from 0 to 1, where a value of 1 indicates complete isotropy, meaning that the material's properties remain consistent regardless of direction.

The behavior of PU foams can exhibit either isotropic or anisotropic characteristics, as investigated in the study by Marvi-Mashhadi, Lopes, and LLorca (2020). In the case of anisotropic foams, the compression response along the directions parallel and perpendicular to the major cell axis is depicted in Figure 9. It is evident that the stress levels decrease by approximately half when transitioning from the parallel direction to the perpendicular direction to the major cell axis.

Figure 9 – Stress-strain relationship for anisotropic foam subjected to compression: (a) parallel and (b) perpendicular

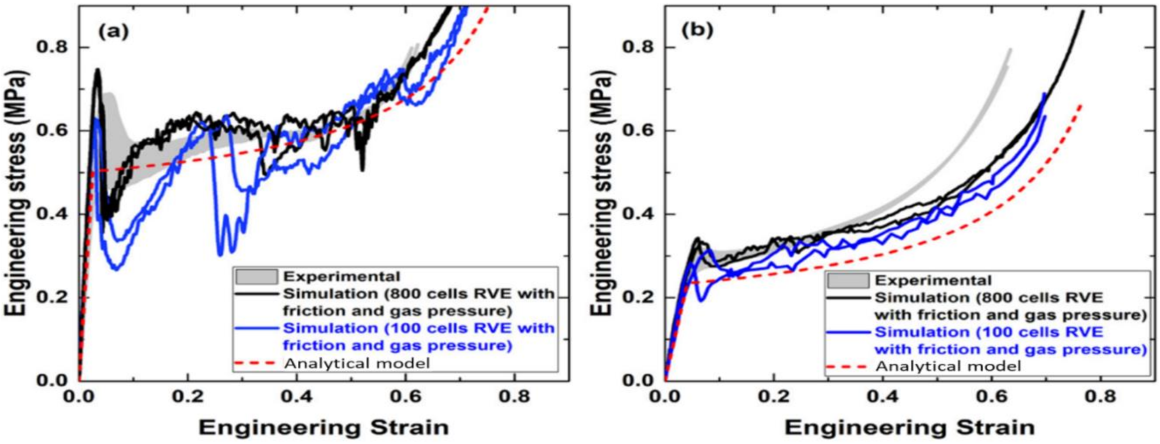

Source: Adapted from Marvi-Mashhadi, Lopes and LLorca (2020).

Mourão and Neto (2002) conducted an analysis of the degree of anisotropy in relation to foam density under compression. Their findings indicate that for foams with densities below approximately 200 kg/m³, the plateau stress and absorbed energy are higher in the direction parallel with the foam growth. In contrast, for PU foams with densities greater than 200 kg/m³, a reversal occurs, with elevated values observed in the direction perpendicular to the foam growth, as depicted in Figure 10.

Figure 10 - Representation of the plateau stress and absorbed energy based on the direction of applied load

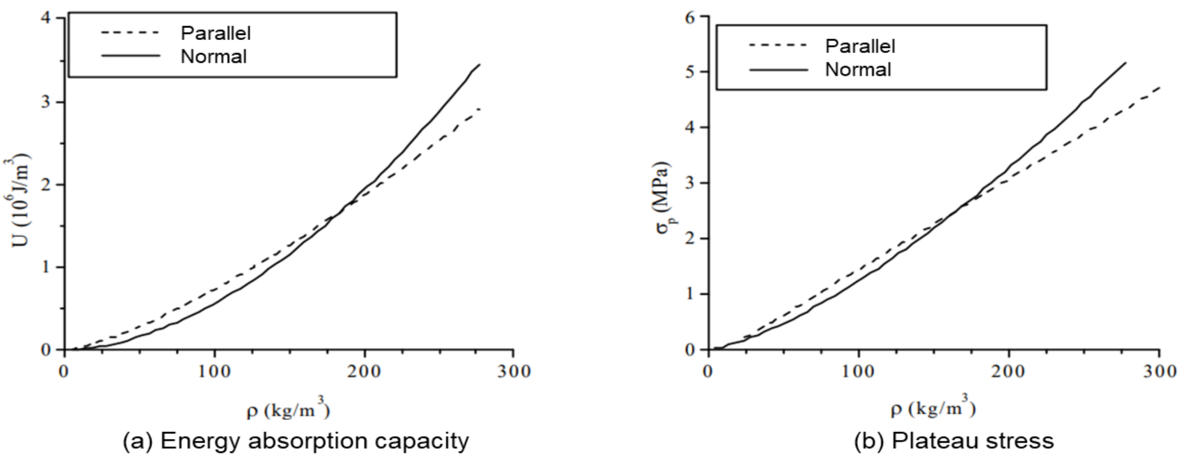

Source: Adapted from Mourão and Neto (2002).

2.2.5 Thermal properties overview

The predominant focus of analysis and research regarding PU foam revolves around its thermal properties, as it serves as an insulation material. While the present study aims to investigate the mechanical behavior of PU foams, it is crucial to comprehend their thermal properties and understand how specific foam characteristics influence thermal performance.

The selection of PU foams as insulation material in refrigerators is substantiated by the findings of Lee and Ramesh (2004). They demonstrate that, in order to achieve the same thermal efficiency as PU foam, other materials would require significantly greater thicknesses. As an example, obtaining the thermal insulation equivalent to a 50mm PU foam necessitates a layer of ceramic bricks with a thickness of 172 cm.

When examining the thermal properties of polyurethane foams, several considerations come into play. Firstly, the cellular morphology, including cell size and foam density, significantly impacts thermal behavior. Furthermore, material properties, such as the thermal conductivity of both the foam material and the gas trapped within the cells, play a crucial role. The overall thermal conductivity (k) of rigid PU foam can be partitioned into three distinct components: the gaseous phase, which predominantly contributes approximately 70% to the total thermal conductivity, the thermal conductivity through the polymeric matrix at 20%, and radiation at 10% (Peyrton; Avérous, 2021).

The thermal conductivity (k) of rigid PU foams exhibits a relationship with foam density. Within the density range of 30 to 50 kg/m³, the foams demonstrate the lowest values of k, indicating enhanced insulation performance. This behavior can be attributed to a favorable balance between the gas phase and the polymeric matrix. However, beyond a density of 50 kg/m³, an increase in foam density leads to a corresponding increase in foam conductivity. This can be attributed to a greater proportion of solid material available for conducting heat within the foam structure (Lee; Ramesh, 2004).

While several factors influencing the properties of rigid PU foams have been addressed, it should be noted that numerous other factors can impact these foam properties. Figure 11 provides a comprehensive overview of these factors and their respective influence on foam properties.

Figure 11 - Overview of factors influencing the properties of rigid PU foams

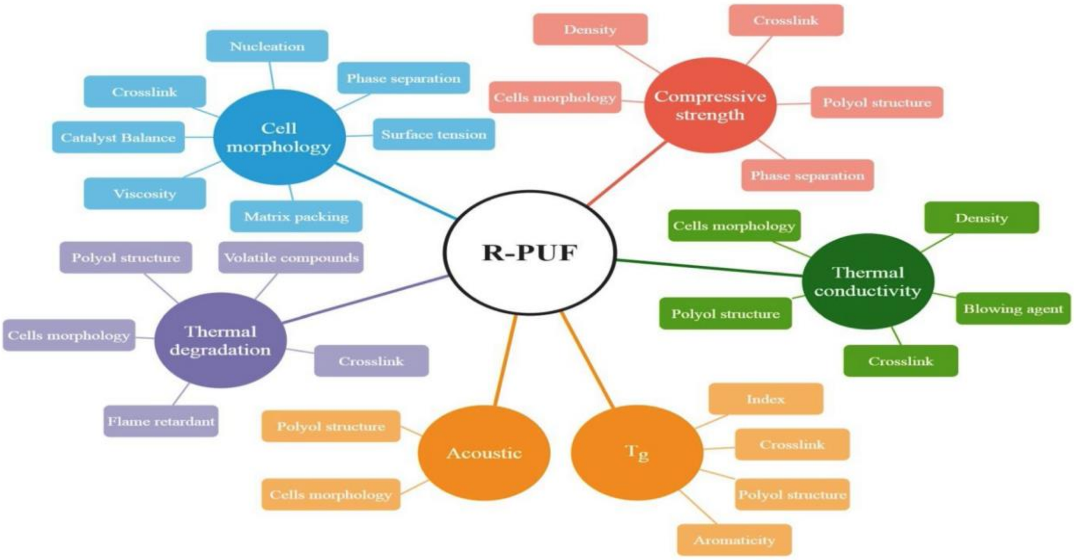

Source: Peyrton and Avérous (2021).

2.3 application of polyurethane in refrigerators

The composition of refrigerator cabinets is an important aspect to consider when analyzing the application of polyurethane in refrigerators. These cabinets consist of an external layer made of thin painted metal sheet and an inner liner made of thermoformed plastic, typically high-impact polystyrene (HIPS) or Acrylonitrile butadiene styrene (ABS) copolymer. The polyol and isocyanate are injected between these two, immediately after mixing, to form the polyurethane foam. This process is illustrated in Figure 12 (American Chemistry Council, Inc., 2021).

Figure 12 - Example of a refrigerator cabinet with highlighted PU foam cross-section

Source: Krauss Maffei (2022).

A review from the perspective of refrigerator applications highlights the high insulation efficiency that allows for the use of thinner thicknesses. As a result, larger internal volumes of products are possible. Additionally, there is mechanical strength that allows for the use of less plastic and steel in the components that make up the products, as well as its adhesive property that aids in the bonding of the internal plastic part with the external metal part (Lee; Ramesh, 2004). Another important characteristic is the ability to fill cabinets even with complex geometries, as can be seen in Figure 12 (Kapps, 2004).

The rigid PU foams used in refrigerators generally have physical properties with a minimum porosity of 95%, low density (30 to 40 kg/m^3), and high compression strength (150 to 200 kPa) (Lee *et al.*, 2017).

In the white goods industry, particularly in the manufacturing of refrigerators, high-pressure foaming machines and molds are utilized. These molds are specifically engineered to accurately reproduce the internal and external geometries of each refrigerator. This design feature ensures that the molds are capable of withstanding the substantial pressures that are generated during the foaming process (Lee; Ramesh, 2004). Figure 13 shows a cabinet after foaming, where the mold and injection machine can be visualized. Figure 14 exemplifies the injection system typically used in the refrigerator industry, showing the tanks and devices up to the injection mixhead (Kapps, 2004).

Figure 13 - Example of a foaming machine and mold for refrigerators

Source: Lee and Ramesh (2004).

Figure 14 - Diagram of a PU foam injection system

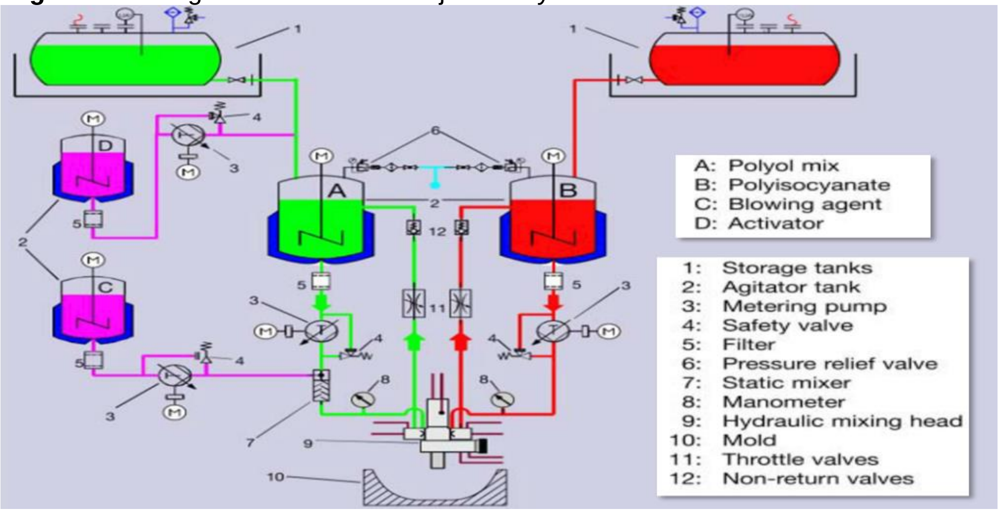

Source: Kapps (2004).

3 MATERIAL AND METHODS

The characterization of the PU foam will involve collecting samples according to the product's characteristics, the process, and the standards. These samples will then be subjected to the sequence of tests indicated throughout the chapter in order to achieve the proposed objectives.

3.1 Sample Collection

Samples of PU foam were obtained from foamed cabinets to conduct tests. To account for the non-homogeneity of PU foam within the cabinets, samples were collected from different regions. Specifically, samples were collected from the top and bottom regions of the cabinet, following the specified dimensions for testing purposes. The selected cabinet features a configuration with an injection point located in the bottom region, aligned with the length of the refrigerator, and upward-facing cavities. In this case, the model in question has the freezer compartment located in the upper region, resulting in a greater available thickness for filling in that area, while the base has the least available thickness for filling. As a result of this difference, it is expected that there will be a discrepancy in the foam filling behavior between the ends of the cabinet, namely, between the top and the bottom. Additionally, considering the expected anisotropy, all samples were labeled according to the direction of foam growth. The samples are illustrated in Figure 15.

Figure 15 - Schematic representation of a two-door cabinet with indication of the sample collection region

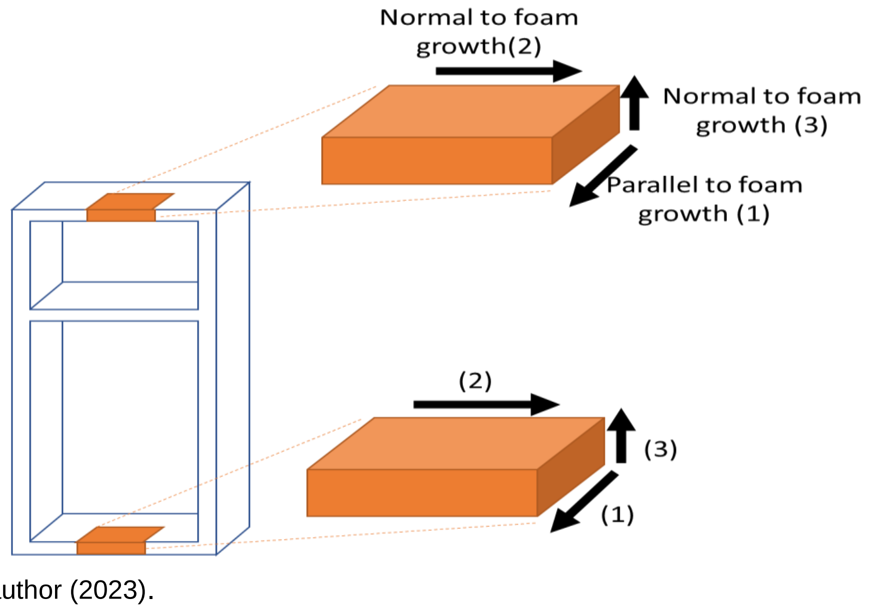

Source: The author (2023).

3.2 Tensile Test

Tensile tests on PU foams were conducted in accordance with ASTM D1623 (2017), with some modifications as follows:

- Due to the dimensions of the products not meeting the sample size requirements specified in the standard, the standard specimen shape was altered while maintaining the proportion of the area supported and by the fracture section in the standard specimen.
- Due to the sample dimensions, it was not possible to apply the recommended device as per the standard. Therefore, the following device was used to secure the samples in the testing machine.

Figure 16 – Tensile device project

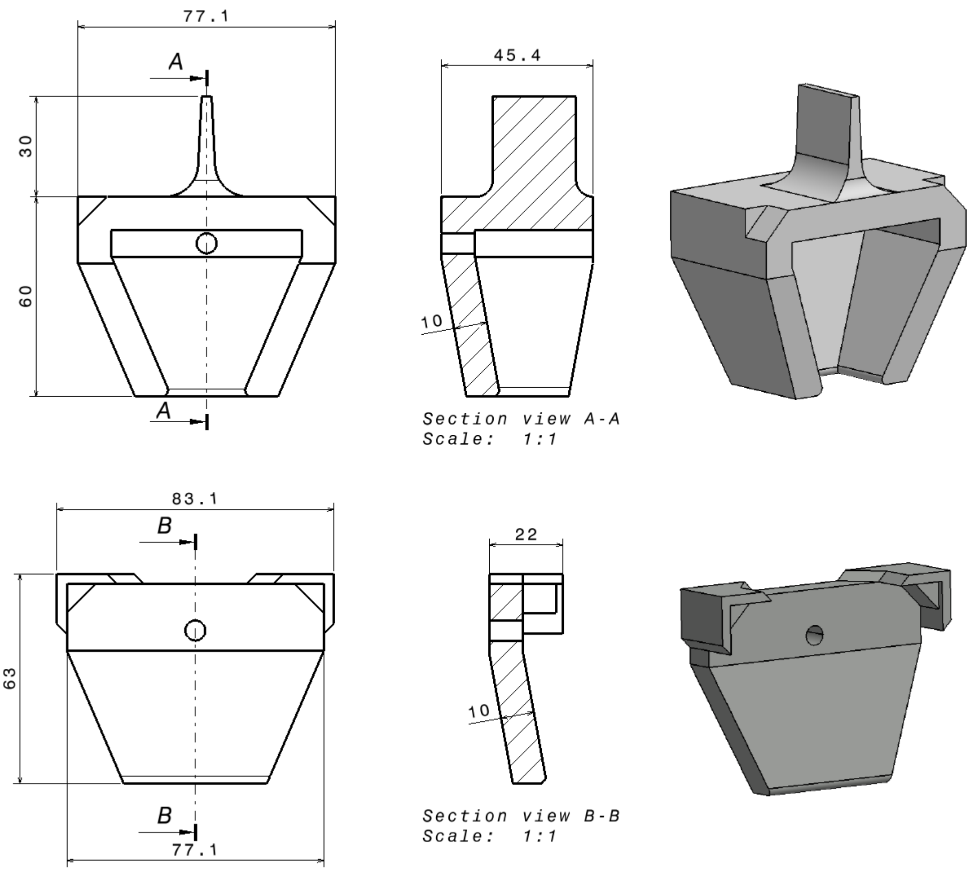

Source: The author (2023).

Figure 17 – Tensile device: (a) 3D project, (b) 3D print prototype, (c) Device in ABS

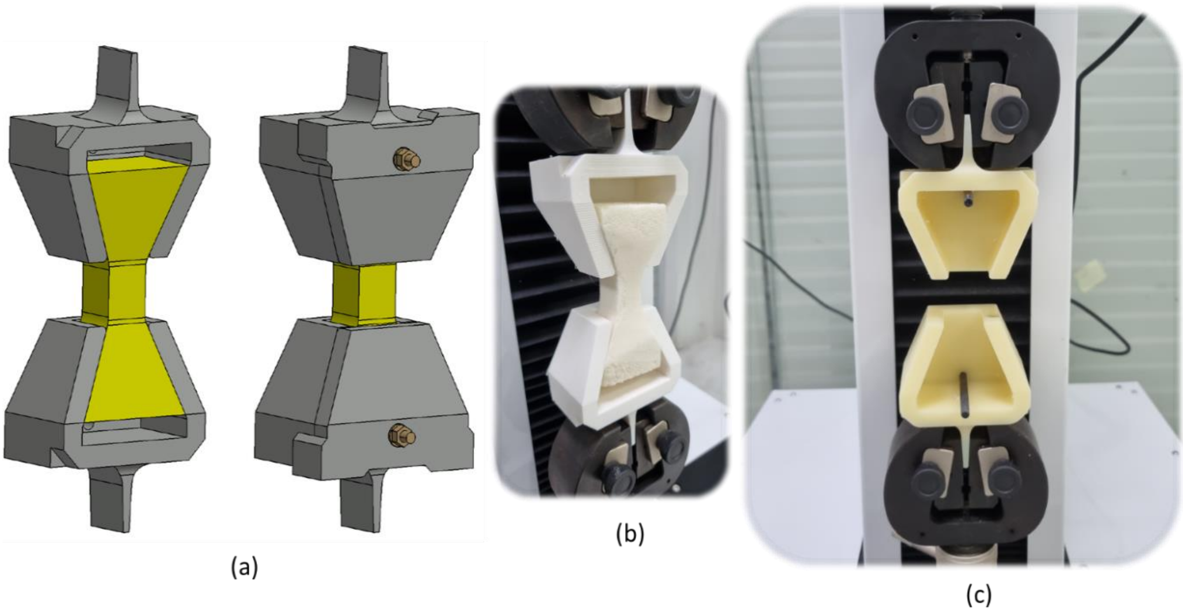

Source: The author (2023).

Figure 18 – Sample dimensional: (a) ASTM D1623, (b) Sample dimensional, (c) Sample

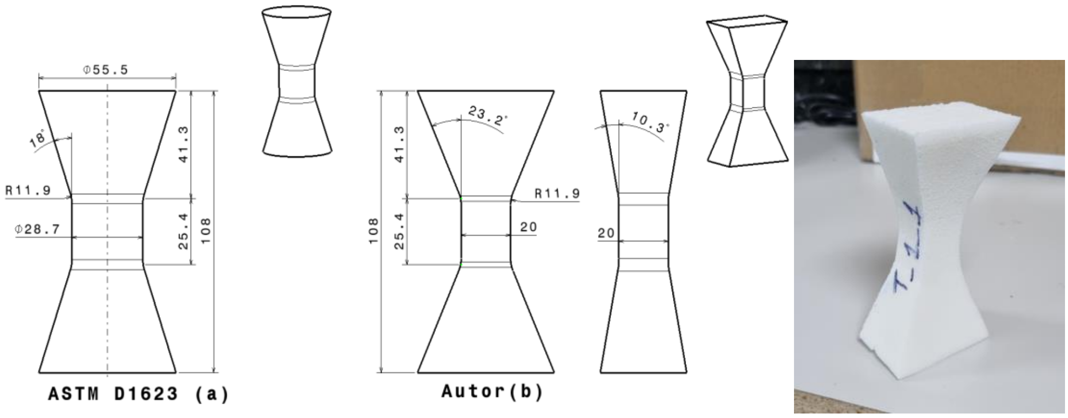

Source: The author (2023).

The testing was conducted using a Biopdi single-column universal testing machine equipped with a 1kN load cell. The test was performed at a speed of 1.3 mm/min, as per the standard recommendation. The samples were labeled in two orientations: perpendicular and parallel to the foam growth, as shown in Figure 15. A total of 5 samples were tested in each orientation, following the sampling tree outlined in Figure 19.

Figure 19 – Sampling tree

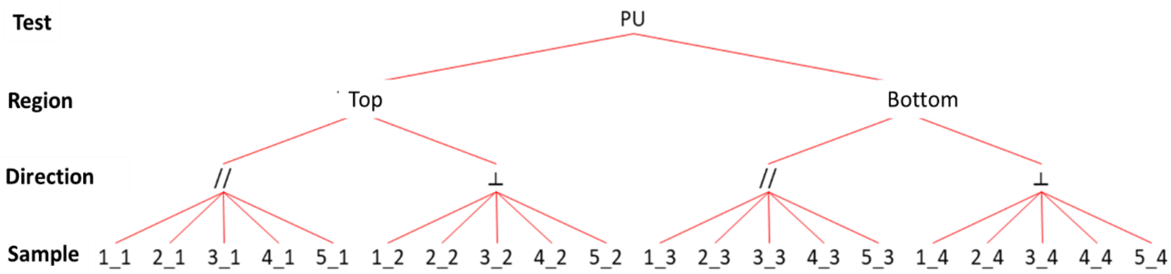

Source: The author (2023).

The stress and strain calculations for the tensile test were performed using the following equations:

$$\sigma = \frac{F}{A_0} \tag{1}$$

Where:

σ = Stress

F = Applied force or load

A_0 = Initial cross-sectional area of the effective part of the specimen

$$\varepsilon = \frac{\Delta l}{L_0} = \frac{L - L_0}{L_0} \tag{2}$$

Where:

ε = Strain

ΔL = Change in length measured between two points

L = Final length

L_0 = Initial length

The modulus of elasticity (E) was determined by calculating the slope of the linear regression line fitted to the stress-strain data.

3.3 Compression Test

The compression testing of PU foams was conducted in accordance with ASTM D1621 (2016). The samples used had dimensions of 50 x 50 x 50 mm. They were divided and labeled in two orientations: perpendicular and parallel to the foam growth. A total of 5 samples were tested in each orientation. Following the study by Xu, *et al.* (2022), the test was performed at a speed of 1 mm/min. The sampling tree for the test followed the same pattern as the tensile test, as depicted in Figure 19.

All measurement points were obtained from the designated origin point, denoted as "O," as depicted in Figure 20. The compressive yield point was determined as "P" if the observed behavior aligned with the characteristics illustrated in Figure 20 right side. Conversely, if the compressive yield point corresponded to the "L" point depicted in Figure 20 left side, it was classified as such.

Figure 20 - Representation of the points on the compression curve

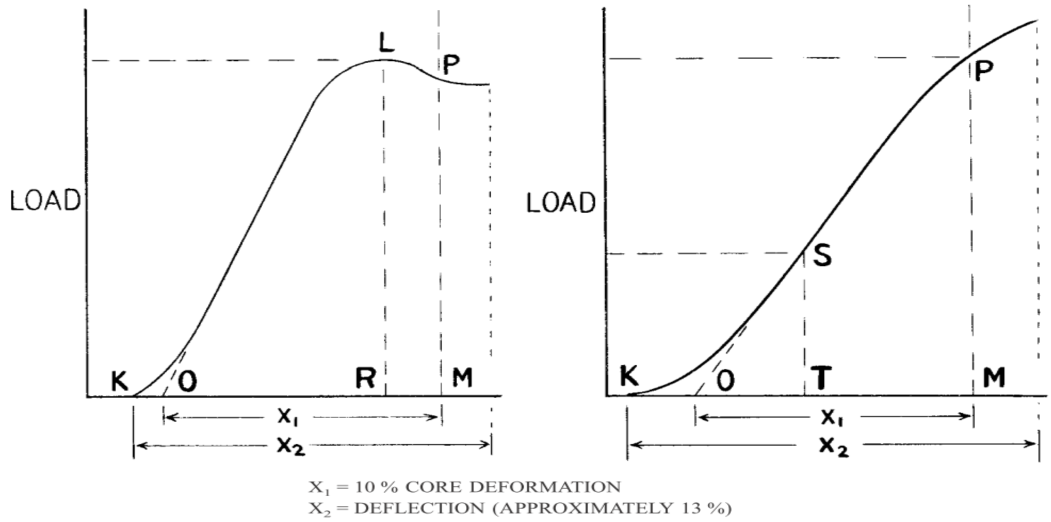

Source: ASTM D1621 (2016).

The compressive strength is determined by dividing the applied load (at point "L" or "P") by the initial cross-sectional area of the sample:

$$\sigma_c = \frac{F}{A_0} \qquad (3)$$

Where:
σ_c = Compressive stress
F = Applied load
A_0 = Initial cross-sectional area of the specimen

To calculate the compressive modulus of elasticity, a reference point (such as point "S" in Figure 20) is established. Using the stress and strain values, the compressive modulus of elasticity is determined by the slope of the line OS in Figure 20:

$$E_c = \frac{\sigma_{c_S} - \sigma_{c_O}}{\varepsilon_{c_S} - \varepsilon_{c_O}} \tag{4}$$

Where:
E_c = Compressive modulus of elasticity
σ_{cS} = Stress at point S
σ_{cO} = Stress at point O
ε_{cS} = Strain at point S
ε_{cO} = Strain at point O

3.4 Three-point flexural Test

The three-point flexural test was conducted in accordance with the method specified in ASTM D790 (2003). The sample dimensions used were 25 x 25 mm with a span length of 100 mm between supports. The samples were separated and labeled in two orientations: perpendicular and parallel to the foam growth. A total of 5 samples will be tested in each orientation. Following the study by Voiconi *et al.* (2013), the test was performed at a speed of 2 mm/min. The sampling tree for the test follows the same pattern as the tensile test, as indicated in Figure 19.

Figure 21 - Three-point flexural test: Diagram (a) and curve (b)

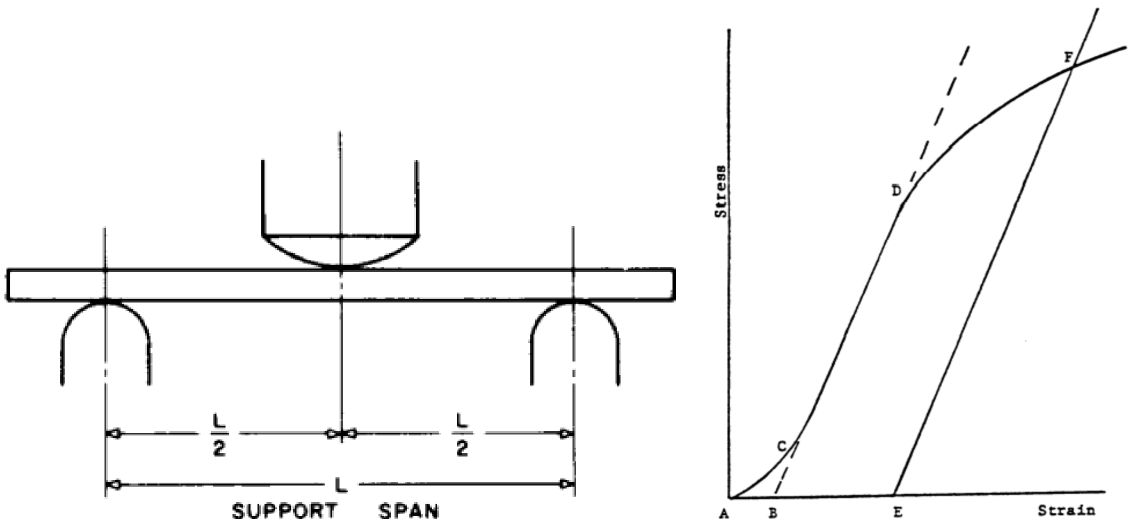

Source: ASTM D790 (2003).

According to the standard, all measurement points should originate from point "B" as indicated in Figure 21. The flexural stress is calculated using the formula:

$$\sigma_f = \frac{3 \cdot P \cdot L}{2 \cdot b \cdot d^2} \quad (5)$$

Where:

σ_f = Flexural stress

P = Applied load on the sample

L = Span length

d = Width of the sample

b = Depth of the sample

The flexural strain is determined by the equation:

$$\varepsilon_f = \frac{6 \cdot D \cdot d}{L^2} \quad (6)$$

Where:
ε_f = Flexural strain in the panel (MPa)
D = Displacement

To calculate the flexural modulus of elasticity, the line BD in Figure 21 is selected. By using the stress and strain values at the endpoints of this line, the modulus is calculated as:

$$E_f = \frac{\sigma_{f_D} - \sigma_{f_B}}{\varepsilon_{f_D} - \varepsilon_{f_B}} \qquad (7)$$

Where:
E_f = Flexural modulus of elasticity
σ_{fD} = Stress at point D
σ_{fB} = Stress at point B
ε_{fD} = Strain at point D
ε_{fB} = Strain at point B

3.5 Sample configuration for tensile, compression, and flexural Tests

A visual guide, represented in Figure 22, illustrates the orientation of each sample and demonstrates the application of load through the use of red arrows.

Figure 22 – Samples configuration

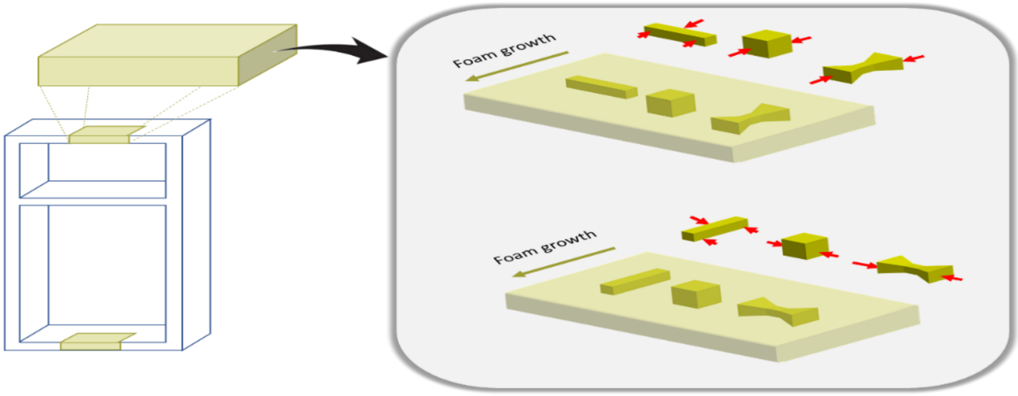

Source: The author (2023).

4 RESULTS

4.1 Tensile Test

The results of the tensile tests are summarized in the following table, which provides the values for maximum stress, maximum strain, and calculated elastic modulus, along with their respective standard deviations.

Table 1 - Summary of tensile test data

		Max Stress (MPa)		Max Strain (%)		Elastic Mod (MPa)	
		Mean	*Std.Dev.*	*Mean*	*Std.Dev.*	*Mean*	*Std.Dev.*
Top	//	0.281	0.031	57.000%	5.099%	0.499	0.072
Top	⊥	0.305	0.032	39.000%	11.358%	0.894	0.226
Bottom	//	0.233	0.035	51.200%	10.569%	0.489	0.136
Bottom	⊥	0.132	0.028	45.600%	17.242%	0.327	0.162
Total		**0.238**	**0.074**	**48.200%**	**12.866%**	**0.552**	**0.259**

Source: The author (2023).

Based on the measured elastic modulus and average maximum strain, the previously described behaviors can be normalized into five distinct curves (average and the four analyzed groups), as represented in Figure 23.

Figure 23 - Stress and strain of PU foams under tensile test: Average, top, and bottom

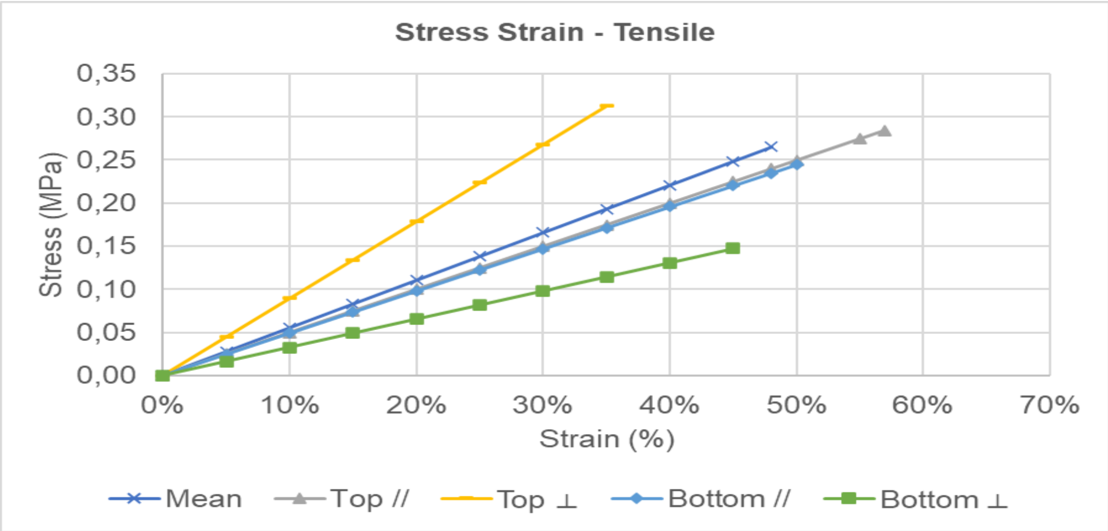

Source: The author (2023).

4.2 Compression Test

The table below presents the results of the compression tests, describing the values of maximum stress, maximum strain, and calculated modulus of elasticity, along with their corresponding standard deviations.

Table 2 - Summary of compression test data

		Max Stress (MPa)		Max Strain (%)		Elastic Mod (MPa)	
		Mean	*Std.Dev.*	*Mean*	*Std.Dev.*	*Mean*	*Std.Dev.*
Top	//	0.138	0.006	8.118%	1.740%	2.425	0.414
Top	⊥	0.136	0.002	6.917%	1.000%	2.598	0.297
Bottom	//	0.100	0.006	10.000%	0.000%	1.740	0.207
Bottom	⊥	0.103	0.007	10.000%	0.000%	2.173	0.266
Total		**0.120**	**0.019**	**8.759%**	**1.631%**	**2.234**	**0.434**

Source: The author (2023).

In Figure 24 below, the average curves of each group and a total average curve are represented.

Figure 24 - Stress and strain of PU foams under compression test: Average, top, and bottom

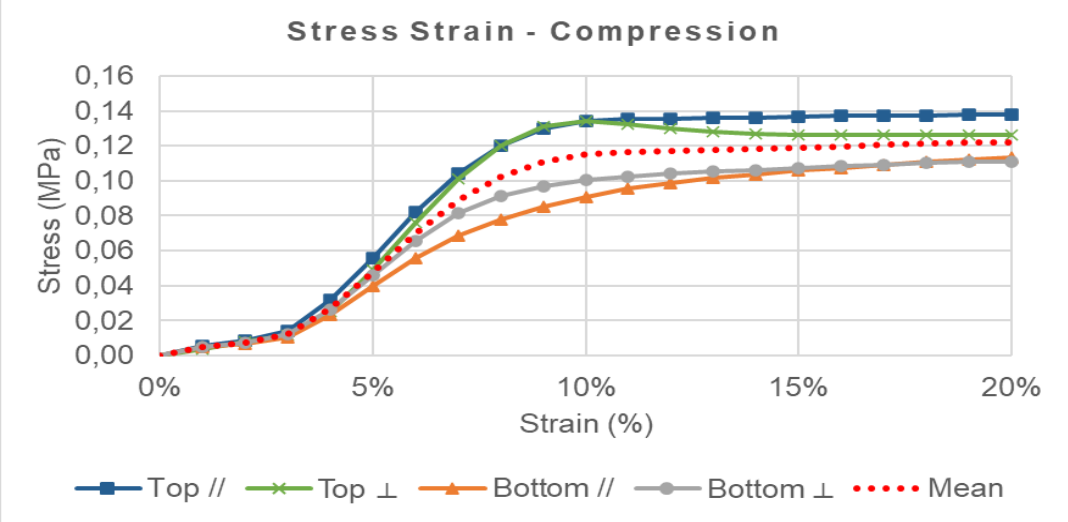

Source: The author (2023).

4.3 Flexural Test

The table below presents the results of the flexural tests, providing information on the values of maximum stress, maximum strain, and calculated modulus of elasticity, accompanied by their respective standard deviations.

Table 3 - Summary of flexural test data

		Max Stress (MPa)		Max Strain (%)		Elastic Mod (MPa)	
		Mean	*Std.Dev.*	*Mean*	*Std.Dev.*	*Mean*	*Std.Dev.*
Top	//	0.298	0.058	27.393%	2.543%	2.359	0.466
Top	⊥	0.273	0.047	22.520%	1.664%	2.368	0.278
Bottom	//	0.275	0.045	19.266%	2.665%	2.054	0.239
Bottom	⊥	0.230	0.067	21.346%	4.550%	1.972	0.721
Total		**0.269**	**0.056**	**22.631%**	**4.145%**	**2.188**	**0.466**

Source: The author (2023).

In Figure 25 below, the average curves of each group and a total average curve are represented.

Figure 25 - Stress and strain of PU foams under flexural test: Average, top, and bottom

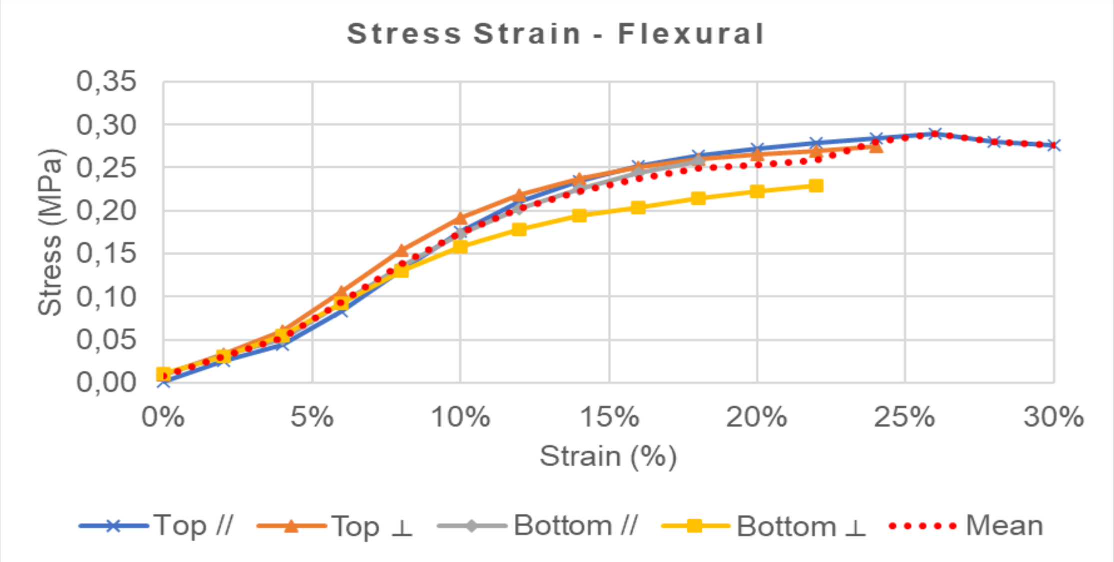

Source: The author (2023).

4.4 Results analysis

This chapter presents some analyzes of the results obtained in an amplified view and together between tests and references.

4.4.1 Effects of PU Foam Factors – Region and Direction

Below are the Pareto charts depicting the effects of location and alignment factors on the characteristics of PU samples in tensile, compression, and flexural tests.

Figure 26 – Pareto charts: tensile, compression and flexural tests

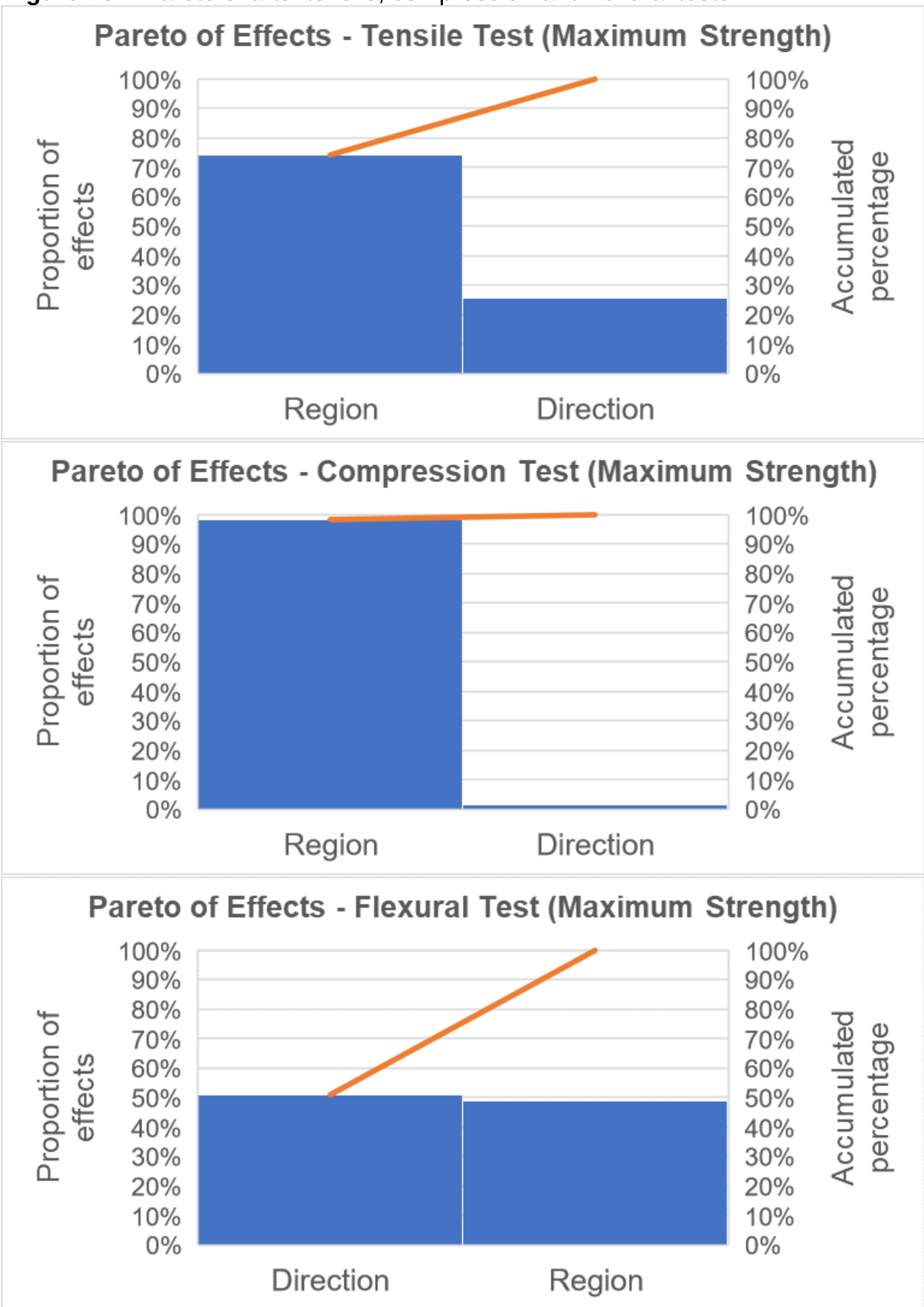

Source: The author (2023).

When considering the effects of the region (top and bottom) and direction (normal and parallel to foam growth) factors, we can identify three distinct groups of behaviors, classified into three levels.

In the first group, corresponding to the lowest level, it is observed that the flexural stress results in low levels of variation between the region and direction factors, indicating that both factors have similar weight.

In the second group, which falls into the intermediate level with greater influence of the factor, we can ascertain that the maximum tensile stress is mainly affected by the region factor, exhibiting approximately 70% of variation compared to direction.

In the third group, corresponding to the highest level, we encounter the maximum effect on the values. Upon analyzing the maximum compressive stress, we observe that the region factor contributes to approximately 98% of the effect on the obtained values.

Therefore, based on the presented data, we conclude that only in the flexural test is it necessary to conduct a more detailed analysis regarding the region and direction factors. For the remaining results, the variations are mainly influenced by the region of the collected samples.

4.4.2 Direction Factor - Analysis between Normal and Parallel

Regarding the direction factor, although the analyses have demonstrated that region has the greatest impact on mechanical properties (except in the flexural test), it is important to examine the direction factor, specifically the degree of anisotropy exhibited by the foams in the three conducted tests.

Comparing the findings with relevant literature on PU foam Marvi-Mashhadi, Lopes, and LLorca (2020), it was discovered that the stress level decreases by approximately fifty percent when transitioning from compression parallel to perpendicular to foam growth. Additionally, Mourão and Neto (2002) indicate that direction parallel to foam growth yields higher strength for densities below 200 kg/m³, albeit at lower levels.

Upon analyzing the obtained results, whether parallel or perpendicular to foam growth, a slight increase in maximum stress was observed when the foam was aligned parallel to its growth direction in the tensile and flexural tests, while the compression test exhibited equal resistance values in both directions. Figure 27 presents this analysis.

Figure 27 – Direction factor - Maximum Strength: Tensile, Compression, and Flexural Tests

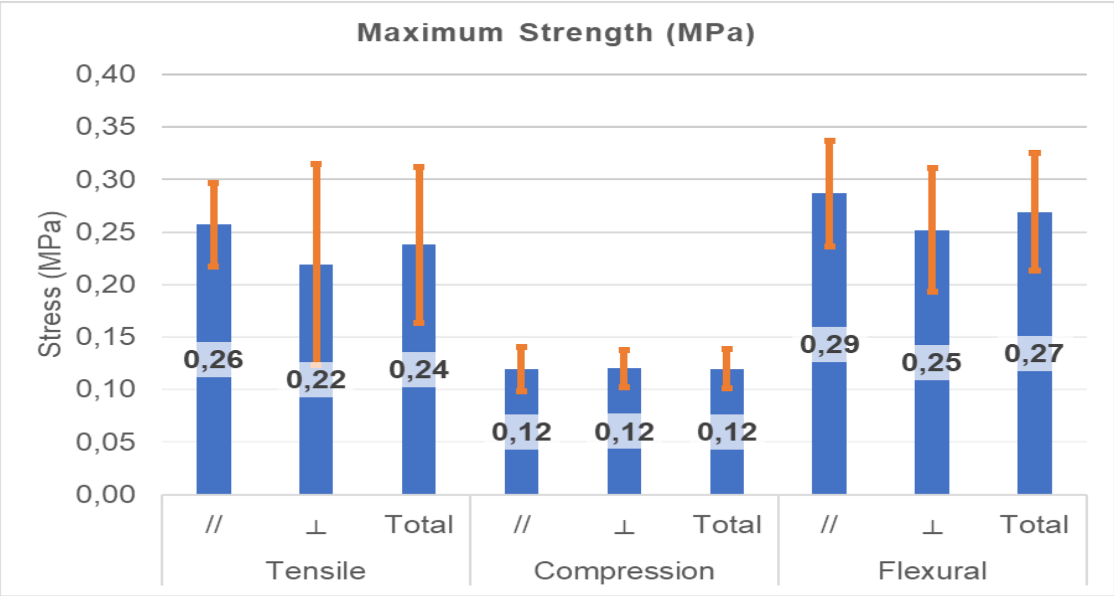

Source: The author (2023).

In this context, when grouping the samples from the top and base and considering only the distinction based on direction, it can be concluded that the polyurethane foam examined in this study demonstrates isotropic behavior under compression, while exhibiting anisotropic behavior under tension and flexion. The degree of anisotropy is depicted in Figure 28 below.

Figure 28 - Degree of Anisotropy: Tensile, Compression, and Flexural Tests

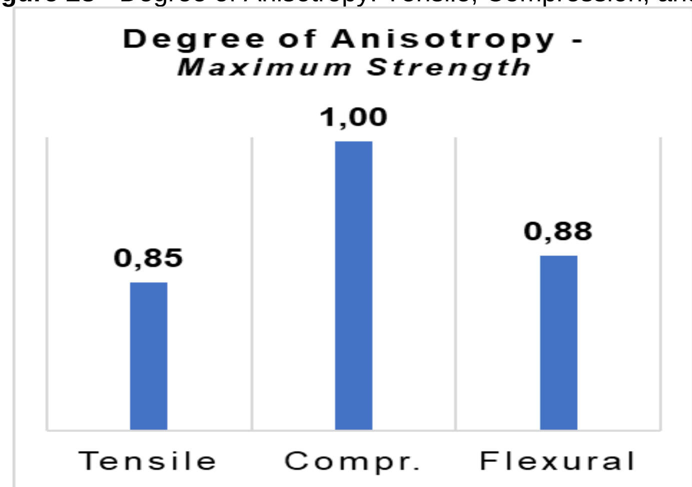

Source: The author (2023).

4.4.3 Region Factor - Analysis between Top and Bottom

Upon examining the obtained results, it was found that the samples collected from the top exhibited superior performance compared to those obtained from the base. This disparity was evident in maximum strength under tensile and compression.

Similarly, when analyzing flexural stress, a similar pattern was observed, albeit on a smaller scale. However, it is important to note that these differences may be confounded by result dispersion, thus preventing a conclusive affirmation of superior performance.

Figure 29 – Region factor - Maximum Strength: Tensile, Compression, and Flexural Tests

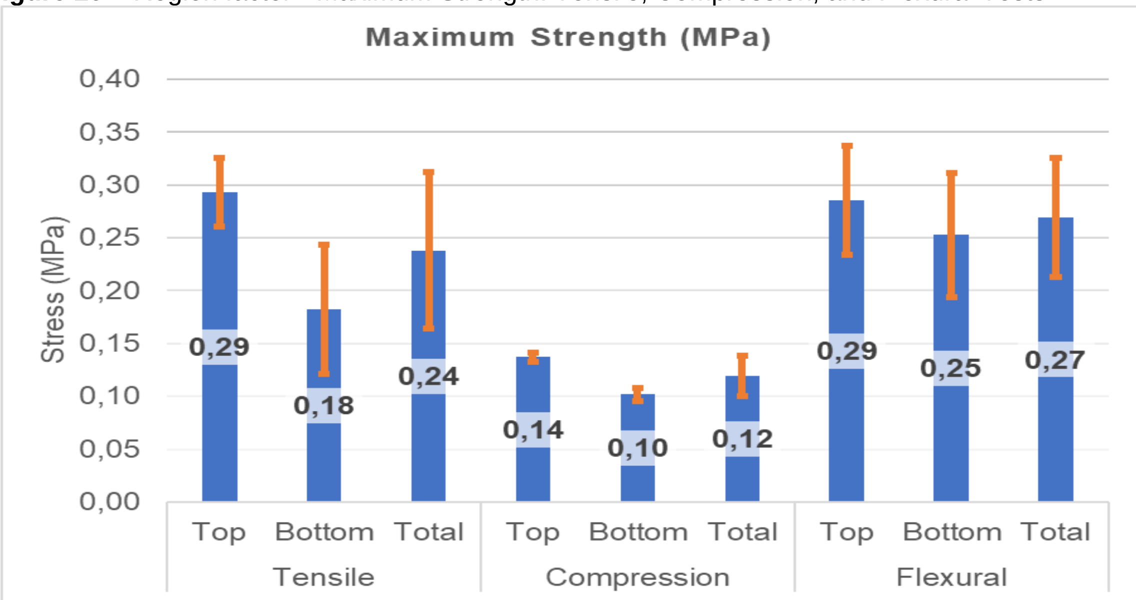

Source: The author (2023).

These results can be explained by the higher incidence of voids, which were identified during the sample preparation process, as shown in Figure 30.

Figure 30 - PU samples (Top and Bottom)

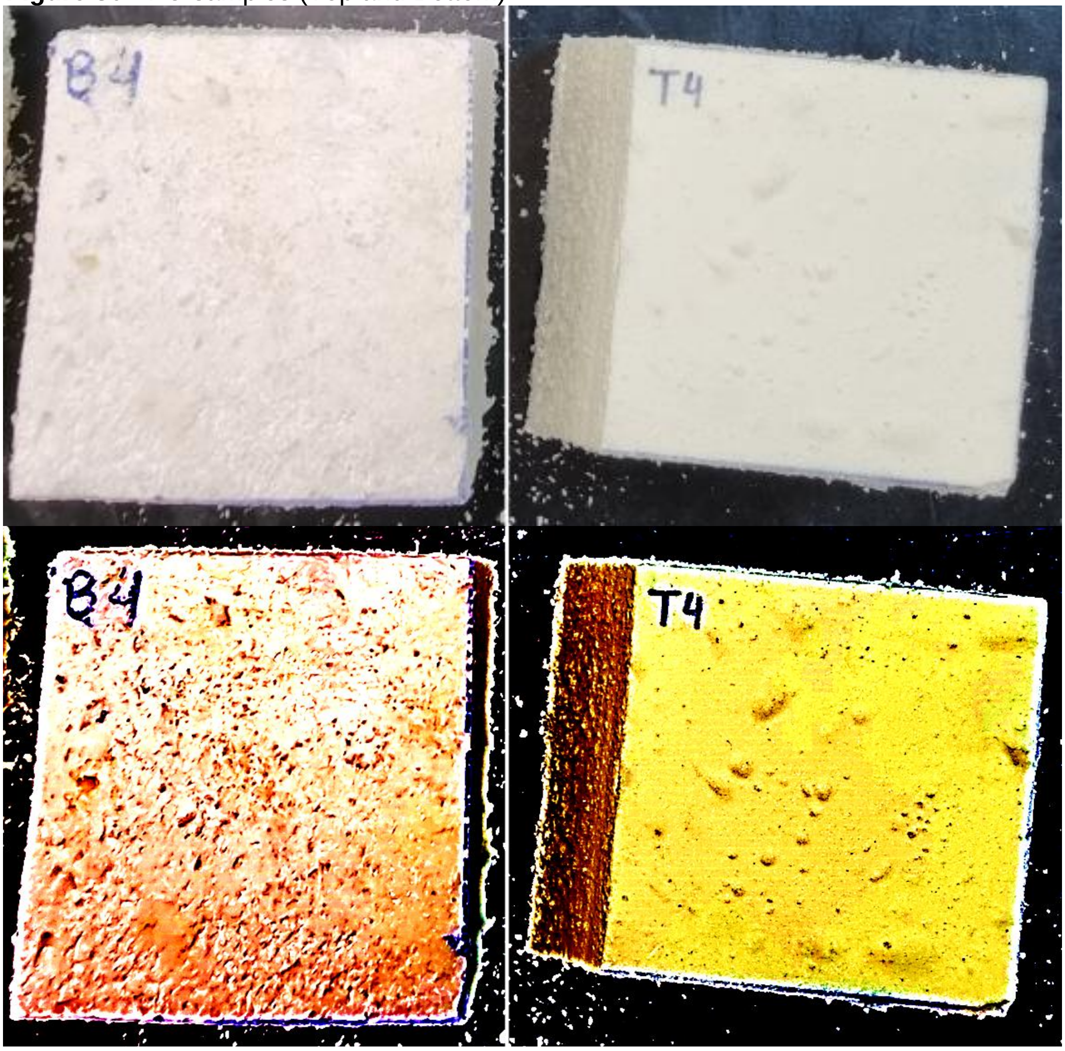

Source: The author (2023).

One possible explanation for the presence of these voids is the entrapment of air during the foaming process. These voids result from a combination of various factors, such as the filling sequence of the cabinet during foaming (which varies according to the available thickness for filling and the configuration of the product cabinet, for example, top freezer or bottom freezer) and the presence of geometries that obstruct the flow of material and foam formation. Nogrid (2023) simulates the effect of configuration and geometry presence in the foaming process using Computational Fluid Dynamics (CFD), and Figure 31 illustrates this air entrapment scenario.

Figure 31 - CFD example of air entrapment in the foaming process

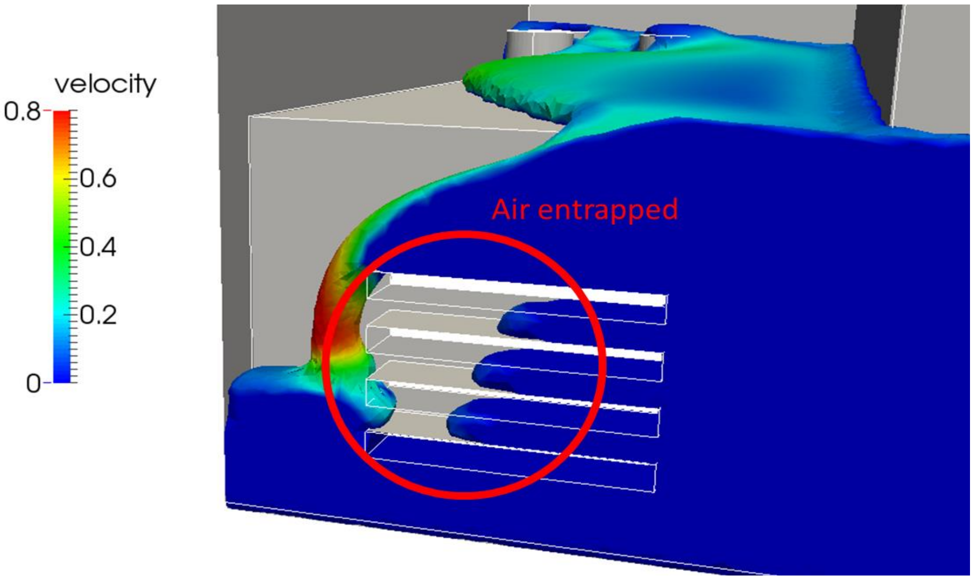

Source: Nogrid (2023).

Furthermore, the positioning of areas for gas escape and the quantity of geometries intended for this escape also play a significant role in this process. To optimize the process and avoid these problems, studies such as Özdemir (2018) are conducted, where the sizing and positioning of gas release areas in a bottom freezer cabinet are analyzed using CFD to identify the best distribution for each case.

Figure 32 - Flow of the foam formation process in a refrigerator

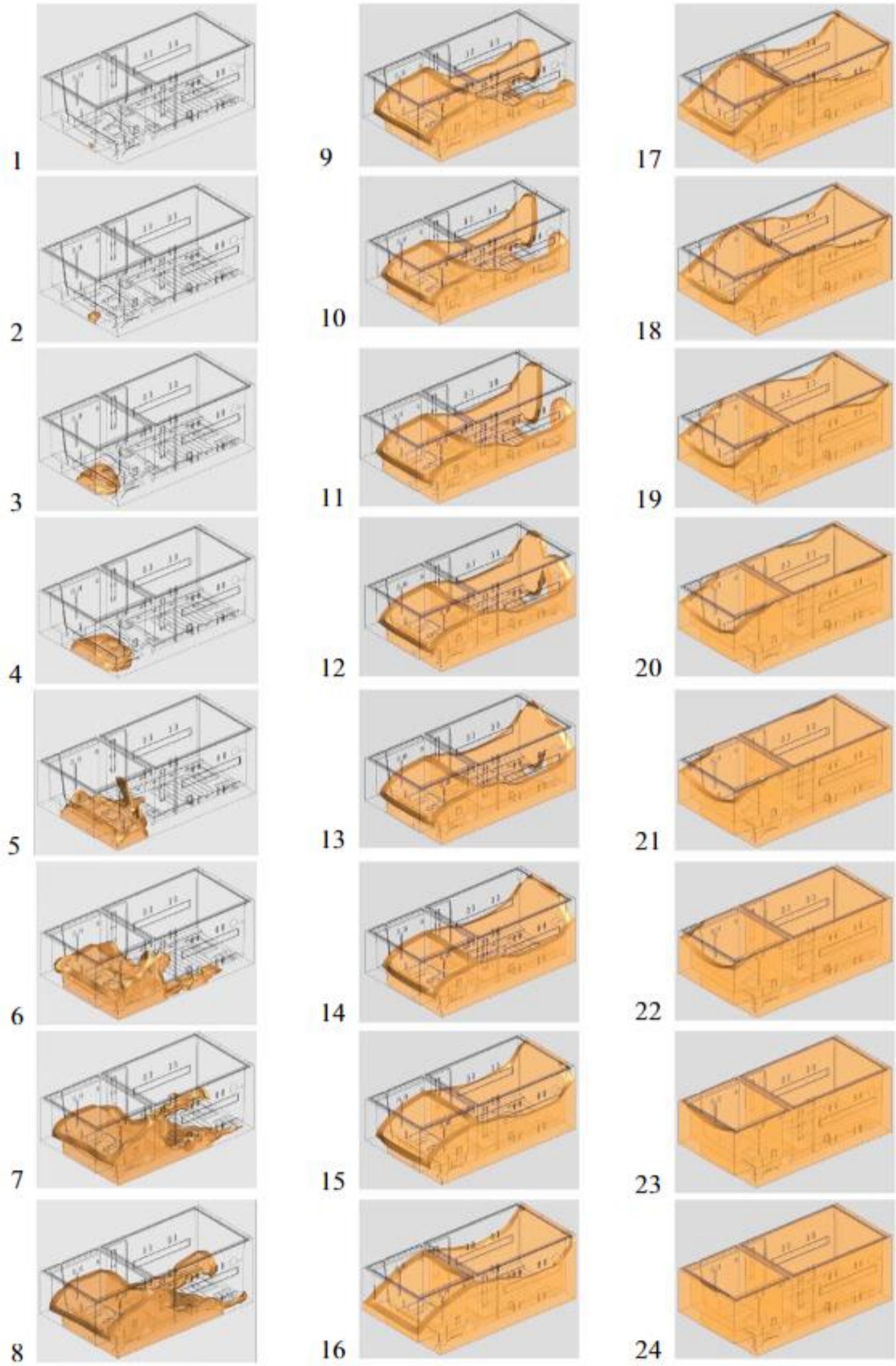

Source: Özdemir (2018).

4.4.4 Compression behavior analysis

The ASTM D1621 (2016) outlines two possible behaviors for rigid cellular plastics under compression, with or without the presence of stress drop, as depicted in Figure 1. When analyzing the compression test curves of the PU foam (Figure 24), both behaviors were observed. In the samples taken from the top perpendicular to the foam growth, a maximum point followed by a stress drop was identified. On the other hand, the remaining curves exhibited the behavior shown in Figure 1 (right side) without the presence of this stress drop. This stress drop occurs due to the rupture of cellular structures, as explained earlier. It was observed that the bottom samples, which have a higher presence of voids, do not provide a stable cellular structure for the PU foam to exhibit this elastic behavior, unlike the top perpendicular to the foam growth samples.

4.4.5 Comparison of properties obtained with other materials composing a refrigerator

Below is a comparison between the maximum stress and modulus of elasticity of the PU foam with high-impact polystyrene (inner liner of the refrigerator) and steel (outer part made of thin painted metal sheet).

Table 4 – Comparison of materials properties

	Maximum Stress (MPa)	**Elastic Modulus (MPa)**
PU Foam – Tensile	0.2	0.6
PU Foam – Compression	0.1	2.2
PU Foam – Flexure	0.3	2.2
High-impact polystyrene (HIPS) (Curbell Plastics, Inc., 2013)	24	2 137
AISI 1010 Steel (MatWeb, LLC, 2023)	365	205 000

Source: The author (2023).

In an absolute analysis of properties, it is observed that PU foam exhibits low strength and modulus of elasticity compared to HIPS and AISI 1010 steel (reference materials). However, further studies are necessary to assess its effect when applied in the refrigerator's structure.

5 CONCLUSIONS

In summary, this research investigated the mechanical properties of PU foam through tensile, compression, and flexural testing. The findings revealed that both the region and direction factors exerted notable influences on the foam's mechanical behavior.

In terms of the region factor, samples obtained from the top portion exhibited superior performance in terms of maximum stress under tension and compression when compared to samples collected from the bottom. These distinctions can be attributed to the presence of voids, which were more prevalent in the bottom samples. Regarding the direction factor, the foam demonstrated isotropic behavior under compression, while displaying anisotropic behavior under tension and flexure. When aligned parallel to the growth direction, the foam demonstrated a slight elevation in maximum stress during the tensile and flexural tests. However, the compression test yielded comparable resistance values in both directions.

Furthermore, a comparative analysis of the mechanical properties between PU foam, HIPS, and steel revealed that PU foam exhibited lower strength and modulus of elasticity. Nonetheless, further investigations are necessary to evaluate the specific implications of PU foam when utilized in the structural context of refrigerators.

These findings make a substantial contribution to the comprehension and application of PU foam across diverse industries, notably in the field of refrigeration. The data acquired from these tests holds significant value for the implementation of Finite Element Analysis to optimize project designs, rectify structural concerns, and potentially cost savings. Through the integration of experimental data and computational analysis, it becomes feasible to enhance the structural efficacy of PU foam-based components, thus realizing more efficient and economically viable solutions. This amalgamation empowers engineers and designers with the ability to make well-informed decisions, ultimately leading to enhanced performance and cost optimization within the realm of PU foam applications.

REFERENCES

AMERICAN CHEMISTRY COUNCIL, INC. **Polyurethanes**. 2021. Available at: https://polyurethane.americanchemistry.com/. Accessed on: 15 June. 2023.

ASTM D1621. **Standard Test Method for Compressive Properties Of Rigid Cellular Plastics**. 2016.

ASTM D1623. **Standard Test Method for Tensile and Tensile Adhesion Properties of Rigid Cellular Plastics**. 2017. DOI: https://doi.org/10.1520/d1623-03

ASTM D790. **Standard Test Methods for Flexural Properties of Unreinforced and Reinforced Plastics and Electrical Insulating Materials**. 2003. DOI: https://doi.org/10.1520/d0790-15

CALIRI JUNIOR, M. F. **Modelos de material para espumas poliméricas aplicadas a estruturas aeronáuticas em material compósito sanduíche**. São Carlos: Universidade de São Paulo - Escola de Engenharia de São Carlos, 2010. DOI: https://doi.org/10.11606/d.18.2010.tde-15082011-223452

CALLISTER, W. D.; RETHWISCH, D. G. **Materials Science & Engineering**. Wiley, 2014.

CURBELL PLASTICS, INC. **High impact polystyrene**. 2023. Available at: https://www.curbellplastics.com/materials/plastics/high-impact-polystyrene/. Accessed on: 10 May. 2023.

KAPPS, D. M. **The production of rigid polyurethane foam**. Insulation - Technical Information, p. 46, 2004.

KIM, T. R. *et al.* Modeling of elasto-viscoplastic behavior for polyurethane foam under various strain rates and temperatures. **Composite Structures**, v. 10, p. 686-695, 2017. DOI: https://doi.org/10.1016/j.compstruct.2017.08.032

KRAUSS MAFFEI. **Insulation foaming for refrigerators**. 2022. Available at: https://www.kraussmaffei.com/en/our-processes/insulation-foaming-for-refrigerators. Accessed on: 10 May, 2023.

LEE, J. H. *et al.* Unified constitutive model with consideration for effects of porosity and its application to polyurethane foam. **Composites Part B**, v. 22, pp. 87-100, 2017. DOI: https://doi.org/10.1016/j.compositesb.2017.11.030

LEE, S.; RAMESH, N. **Polymeric foams**: mechanisms and materials. Washington, D.C.: CRC Press LLC, 2004.

MARVI-MASHHADI, M.; LOPES, C.; LLORCA, J. High fidelity simulation of the mechanical behavior of closed-cell polyurethane foams. **Journal of the Mechanics and Physics of Solids**, v. 135, n. 1, 2020. DOI: https://doi.org/10.1016/j.jmps.2019.103814

MATWEB, LLC. **AISI 1010 Steel, cold drawn**. 2023. Available at: https://www.matweb.com/AISI 1010 Steel. Accessed on: 10 June, 2023.

MOURÃO, R. P.; MATTAR NETO, M. Caracterização de espuma polimérica para uso em embalagens para transporte de rejeitos radioativos. *In:* CONGRESSO NACIONAL DE ENGENHARIA MECÂNICA, 2., 2002. DOI: https://doi.org/10.20906/cps/con-2016-1458

NOGRID. **Simulation of three Refrigerator PUR Filling and Foaming Processes.** 2023. Available at: https://www.nogrid.com/article/three-pur- foaming-refrigerator-filling-processes. Accessed on: 20 February, 2023.

ÖZDEMIR, İ. P. Effects of air vents on the flow of reacting polyurethane foam in a refrigerator cavity. **Adv Polym Technol,** p. 2420-2428, 2018. DOI: https://doi.org/10.1002/adv.21916

PEYRTON, J.; AVÉROUS, L. Structure-properties relationships of cellular materials from biobased polyurethane foams. DOI: https://doi.org/10.1016/j.mser.2021.100608

VOICONI, T. *et al.* **Determination of Flexural Properties of Rigid PUR Foams Using Digital Image Correlation**. Solid State Phenomena, 2013. DOI: https://doi.org/10.4028/www.scientific.net/ssp.216.116

WITKIEWICZ, W.; ZIELIŃSKI, A. Properties of the polyurethane (PU) light foams. **Advances in Materials Science**, v. 6, n. 2, 2006.

XU, G. *et al.* A nonlinear constitutive model of rigid polyurethane foam considering direction-dependence and tension–compression asymmetry. **Construction and Building Materials**, v. 339, 2022. DOI: https://doi.org/10.1016/j.conbuildmat.2022.127540

Os autores:

João Paulo Soares Kaiser
Possui graduação em Engenheira Mecânica pela Universidade Federado do Paraná (2017). Experiencia em desenvolvimento de produtos e engenharia de manufatura. Proficiente em desenvolvimento e gerenciamento de projetos.

João Morais da Silva Neto
Graduou-se em Engenharia Mecânica pela Universidade Federal do Pará (1995), Mestrado em Engenharia Mecânica na Universidade Federal de Santa Catarina, na área de vibrações e acústica (1999) e Doutorado em Engenharia Mecânica (2004) na mesma universidade. Possui experiência em análise modal experimental, no controle passivo de vibrações pela inserção de materiais viscoelásticos e em caracterização dinâmica de materiais viscoelásticos. Com mais de dez anos de experiência em pesquisa e desenvolvimento do setor industrial, desenvolveu trabalhos na área de viscoelasticidade não-linear, mais especificamente em modelagem e caracterização de dados para modelos hiperelásticos, submetidos a grandes deformações. Trabalhou com modelagem de elementos finitos utilizando softwares comerciais tais como, ABAQUS e ANSYS. Tem objetivado nas suas investigações um melhor entendimento dos métodos de caracterização dinâmica de materiais viscoelásticos, na aplicação desses em controle de vibrações e ruído, na representação adequada por via de modelos do amortecimento material, em análise modal experimental, na obtenção dos parâmetros de modelos hiperelásticos, com vistas a simulação via método dos elementos finitos.

Harrison Lourenço Corrêa
Possui graduação em Engenharia Química pela Universidade do Estado do Rio de Janeiro (2004), Mestrado em Química pela Universidade do Estado do Rio de Janeiro (2008) e Doutorado em Química pela Universidade do Estado do Rio de Janeiro (2015). Atualmente é Professor Associado da Universidade Federal do Paraná. Tem experiência na área de Engenharia Química, com ênfase em Materiais Poliméricos, atuando principalmente nos seguintes temas: Economia circular, reciclagem de polímeros e reologia de materiais. É membro da Sociedade Internacional para o Desenvolvimento e Sustentabilidade e revisor de importantes revistas internacionais na área de Sustentabilidade Ambiental e Materiais Poliméricos, atuando como parecerista para Springer Nature, Frontiers, SAGE Publishing, dentre outras. É coordenador do Laboratório de Estudos sobre Economia Circular e Sustentabilidade, LaCESS (Laboratory for Circular Economy and Sustainability Studies).

Artigo recebido em: 17/07/2023 e aceito para publicação em: 02/08/2023
DOI: https://doi.org/10.14488/1676-1901.v23i1.4953